Proceedings of the 2006 IASME/WSEAS International Conference on Continuum Mechanics, Chalkida, Greece, May 11-13, 2006 (pp38-43)

The flow through an orifice of semi-rigid-polymer solutions

GEORGE PAPAEVANGELOU
Department of Rural and Surveying Engineering, Faculty of Engineering,
Aristotle University of Thessaloniki, Thessaloniki 54006,
GREECE

Abstract: -The orifice flow of scleroglucan solutions is studied. Under given conditions, this molecule behaves as a semi-rigid rod in solutions. Solutions in glucose-water syrups were examined, which show considerable vortex growth in orifice flow depending on flow regime and concentration. The vortex reattachment length is studied as a function of regime and concentration. The flow curves in orifice flow are characterized by a linear pressure drop – flow rate relation. The extensional viscosity is derived from the orifice flow data by the Binding analysis. Comparison with the Batchelor analysis for closely spaced fibers is satisfactory if molecular extension as well as alignment along the streamlines is considered.

Key-words: semi-rigid polymers, solutions, suspensions, flow through an orifice, extensional properties

1 Introduction

Flexible polymer solutions have been quite thoroughly studied, as shown in a recent review paper by Larson [1] as well as in a paper by Prakash [2]. This is not the case for rigid polymer solutions which are much less elastic. They are expected to behave like suspensions of rigid slender particles. For the latter, constitutive equations are available in the dilute range by Hinch and Leal [3-5]. The range of semi-dilute systems has been examined by Batchelor [6] for extensional flows. Different extensions based on the micromechanics of ellipsoidal particles have been proposed by Dinh and Armstrong [7] and Lipscomb et al [8].

Many authors have been interested in the experimental flow properties of rigid slender particle solutions. Mewis and Metzner [9] studied solutions of glass fibers and verified the Batchelor analysis.

Attention was given also to contraction flows of such systems. Binnington and Boger [10] showed constant vortex length. They thus stressed the point that for semi-rigid rod systems, extensional viscosity should be independent of the extensional rate.

Lipscomb et al [8] developed a numerical model for the contraction flow under inertialless conditions. A key assumption in this model is that fibers align with streamlines. Numerical simulation results were compared to experiments with glass fibers suspended in a viscous syrup. Good agreement was observed for the flow field structure and the variation of the reduced vortex reattachment length X with the different parameters: It increases with fiber concentration for a given aspect ratio.

Chiba et al [11] presented numerical results that agreed with those of Lipscomb et al [8], and extended them by considering the effect of inertia. Concentration was again shown to increase the vortex length and inertia to crush the vortices. It was also supposed that the length of the vortex is independent of the flow rate when fibers of polymer molecules do not change their configuration.

Keiller et al [12] established the way vortex enhancement varies with concentration. Keiller and Hinch in their analysis [13], find that the vortices should decrease with concentration. They suggested that the vortices observed previously result from the contraction flow and not the flow singularity.

Mongruel and Cloitre examined the orifice flow of semi-dilute solutions of polyamide fibers [14] as well as xanthan [15]. They showed [14] that the vortex length can reach one upstream diameter. In [15] they study in detail the pressure drop effect resulting in Trouton ratio values of up to 100.

The above studies show that flow-induced orientation of slender rigid bodies may generate considerable extensional effects. In contraction flows this results in viscoelastic vortices that seem to be flow rate independent in the regimes examined. It should be expected that at lower flow regime conditions, where particle orientation should be random, contraction flow should resemble to that of a newtonian fluid, with concave corner vortices. The evolution from the newtonian corner vortices to the flow-rate-independent viscoelastic vortices and the effect of extensional properties on the excess pressure drop need further research.

In the present paper, we present orifice flow experiments with solutions of scleroglucan. The objective is to study extensional effects generated in this geometry and to confront observations with predictions on the extensional viscosity from slender rigid body theories and orifice flow analysis.

In the following section we describe the polymer, the fluids and their shear viscosity. In sec. 3 the determination of the concentration ranges is discussed. Sec. 4 treats the orifice flow of the solutions in non-inertial conditions. In sec. 5, the extensional viscosity is discussed, derived from the orifice flow data and independent model predictions.

2 The fluids and their shear viscosity

The fluids were solutions of scleroglucan, a polysaccharide similar to xanthan and to schizophylan, provided by Elf Sanofi in powder form, with a reported molecular weight of $5 \cdot 10^6$. Nardin and Vincendon [16] have shown a that it has a triple helical structure. They have also shown that, when dissolved in DMSO, the molecule is dispersed to take up a single-chain random-coil conformation.

Yanaki et al [17] found that its intrinsic viscosity is 243 cm^3g^{-1} in DMSO (flexible chain), but in 0.01N NaOH it obtains much higher values ($6.6.10^3$ cm^3g^{-1}) since it is rodlike. Yanaki and Norisuye [18] found in the latter solvent a contour length of h=0.3 nm, a diameter of trimmer rod of 2.5 nm and an $[\eta_0]$ of $4.4 \cdot 10^3 cm^3g^{-1}$. Noik and Lecourtier [19] found an $[\eta_0]$ of $9200 cm^3g^{-1}$ for aqueous solutions.

The above-mentioned literature data indicate that in a solution, it can behave either as a rigid or as a flexible polymer, depending on the solvent. For a molecular weight close to ours, its intrinsic viscosity may vary from, $240 cm^3g^{-1}$ (as flexible) up to $10^4 cm^3g^{-1}$ (as rigid).

Glucose/water syrups were used here as solvents, in order to avoid high shear-thinning and inertia [20]. Solutions of concentrations of 100, 500 and 5000ppm (w/w) were prepared in a solvent of 80/20 glucose/water as well as a solution of 2000 ppm in a thicker syrup (90/10)(tab. 1).

The shear viscosity of the solutions was measured by the CarriMed Controlled Stress Rheometer. A cone-plate geometry has been used with a cone angle of 1° and a diameter of 6cm. All measurements (fig. 1) were carried out at 20°C. No shear-thinning was detected for the 100 ppm solution. Its constant shear viscosity is η=1.27 Pas. Slight shear-thinning can be observed for the 500 ppm solution. For $\dot{\gamma} > 1$ s^{-1} it behaves as a power-law fluid. Its zero shear viscosity is 1.85 Pa·s. The 2000 and 5000 ppm solutions are more shear-thinning. As the content in glucose is higher in the 2000 ppm fluid, this later has a higher viscosity from the 5000 ppm one. Their zero-shear viscosities are 19.5 and 15.5 Pa·s respectively.

The intrinsic viscosity is estimated to be: $[\eta_0]$ = 580 cm^3g^{-1}, indicating an intermediate situation between rigid and flexible structures. Table 1 reports the shear data of the solutions, where η_{solv} is the solvent viscosity, c_v the volume concentration and λ the characteristic time evaluated as will be shown later on, to correspond to the rotational relaxation time. The coefficients k and m referred in the last two columns of the table, correspond to the power law:

$$\eta_s = k \cdot \dot{\gamma}^{m-1} \qquad (1)$$

Table 1. Shear data for the glucose syrup solutions.

c (ppm)	Gluc. (%)	η_0 (Pas)	η_{solv} (Pas)	c_v (g/l)	λ (sec)	k of eq.1	m of eq. 1
100	80	1.3	1.2	0.136	0.032	1.3	0
500	80	1.9	1.2	0.68	0.823	1.85	-0.03
2000	90	19.5	5.0	3.0	101.6	13.68	-0.06
5000	80	15.5	1.2	6.8	79.6	8.0	-0.17

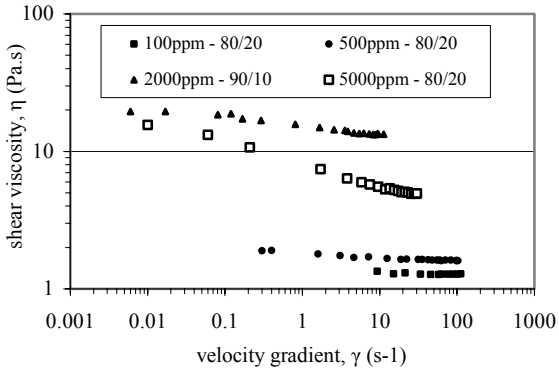

Fig. 1. The steady shear viscosity.

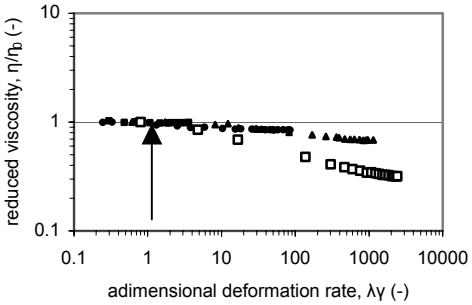

Fig. 2. The reduced shear viscosity.

3 Concentration ranges

Doi and Edwards [21] classify the solutions of rodlike polymers into four concentration regimes. Denoting by L the length of the rods, b their diameter, c_v the weight per volume concentration and n the number of polymers per unit volume:

$$n = c_v \cdot \frac{N_A}{M} \qquad (2)$$

the classification of [21] is shown in table 2:

Table 2. Concentration ranges [21].

dilute		Semi-dilute		Conce-ntrated		Liquid Crystal.
Free rotation	$n_1=L^{-3}=6.7\mu m^{-3}$	Severe restricti on of rotation	$n_2=b^{-1}L^{-2}=1210\mu m^{-3}$	Excluded volume interactions important in both static and dynamic properties	$n^* > n_2$	Polymers aligned, anisotrop ic liquid

Regime transitions are smooth, so n_1, n_2 and n^* are indicative values for progressive changes in the solution properties. For our polymer, the diameter is close to 3nm [18, 19]. From the calculated intrinsic viscosity we find L=0.53μm and L/b=180.

The limits of the concentration ranges are then: n_1=6.72μm^{-3} and n_2=1210μm^{-3}. For our lowest and highest concentration solutions, n is 16.4 and 820μm^{-3} respectively, which indicates that the all our solutions are situated in the semi-dilute range.

In the dilute range, the rotational relaxation time for dilute solutions is given by [21]:

$$\lambda_{r0} = \frac{1}{2D_r} = \frac{\pi \cdot \eta_s \cdot L^3}{6 \cdot \left(\ln\left(\frac{L}{b}\right) - \gamma \right) \cdot k_B \cdot T} \quad (3)$$

where k_B is the Boltzmann constant, D_r is the rotational diffusion constant and γ=0.8 a correction factor. For semi-dilute solutions, the rotational relaxation time is larger than in dilute solutions by a factor:

$$\frac{\lambda_r}{\lambda_{r0}} = \frac{\left(n \cdot L^3\right)^2}{\beta} \quad (4)$$

where β is a correction factor of the order of 10^3.
The relaxation time for each solution is shown in table 1. The adimensional shear viscosity was then plotted versus the reduced deformation rate (Fig. 2). The onset of shear-thinning occurs at $\lambda \cdot \dot{\gamma} \cong 1$, which is an indication that the obtained λ values characterize fluids' properties.

4 The orifice flow

4.1 The flow curves

Orifice flow experiments were performed in submerged and free jet configurations (upstream length 150mm, upstream and downstream diameters 20mm), at temperatures between 20.3 and 21.5°C.
These configurations are described in detail in [20]. Two orifices of respective diameters 1.2 mm and 0.53 mm were used. A conical channel was formed by the main flow region, as expected. No deviation from the slope 1 can be detected in the flow curves (Fig. 3), which is in very good accordance with similar experiments of Mongruel and Cloitre [15] as well as with Cartalos and Piau [22].

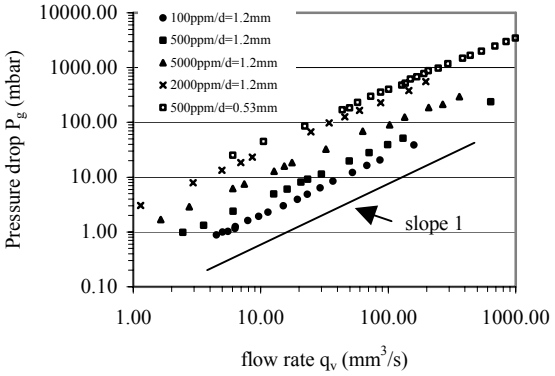

Fig. 3. The flow curves of the solutions.

The flow curves were represented in a dimensionless way, by the use of the coefficient C′:

$$C' = \frac{P_g}{P_N} = \frac{P_g}{\frac{3}{4}\pi \cdot \eta \cdot \dot{\gamma}} \quad (5)$$

which denotes the ratio of the pressure loss to that necessary to push through the orifice a newtonian fluid of the same viscosity. The deformation rate:

$$\dot{\gamma} = 8 \cdot \frac{3m+1}{m} \cdot \frac{q_v}{\pi d^3} \quad (6)$$

has been shown to represent very well orifice flow data [20]. In the case of suspensions of slender rigid particles, particle alignment with flow should be considered for the calculation of η in eq. 5. In our case, molecules are submitted to an extensional field that is very efficient in orienting particles and so, $\eta=\eta_s$ was taken in eq. 5.
The value of C' increases with concentration, staying in the range 1-6, which is in good agreement with respective observations in [15].
Two regimes of constant values of the coefficient C' can be distinguished (Fig. 4), for the 100ppm solution: an initial newtonian regime at low flow rates where C' is close to 1 and the flow field is like the one for a newtonian fluid, and a higher regime where C' is constant indicating a constant extensional viscosity from the Binding analysis [23] and the flow field is characterised by an elastic convex vortex.
An intermediate regime exists between these two regimes where C' is increasing. During the first newtonian regime, molecules are uniformly oriented. During the intermediate transition regime they start to be oriented by the flow. The final higher regime finds them fully aligned.
For the l00ppm solution deviation from the newtonian regime occurs at $\lambda \cdot \dot{\gamma}$=3.5. The final regime is reached for $\lambda \cdot \dot{\gamma}$=10. For more concentrated solutions, where $\lambda \cdot \dot{\gamma}$>10, the final regime of constant C' is only observed. The difference observed between the two diameters for the 500ppm solution was due to the fact that the measurements at high regimes with the d=0.53mm orifice have been influenced by inertia as will be shown later on.

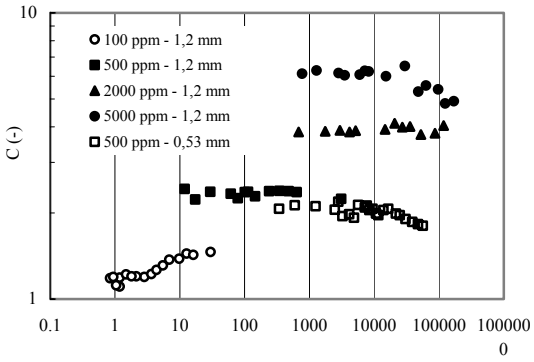

Fig. 4. Dimensionless representation of the flow curves.

4.2 The vortex re-attachment length

By visualizing the flow and taking pictures of it, measurements of the vortex reattachment length:

$$X = \frac{L_v}{D_u} \quad (7)$$

were carried out, where L_v is the length of the vortex and D_u=20mm the upstream tube diameter. The evolution of the reduced re-attachment length of the vortex X is shown in Fig. 5. For the 100 ppm solution, X reaches a constant value X_∞ at $\lambda\cdot\dot{\gamma}=3.5$, close to the onset of the transition regime. As concentration is increased, the value of $\lambda\cdot\dot{\gamma}$ where X_∞ is reached, increases. On the flow of the 500 ppm solution, X is decreasing under the influence of inertia. The sudden increase of the vortex height seems to be triggered in the same $\lambda\cdot\dot{\gamma}$ value for the two lowest concentration solutions. For the two highest concentration solutions, the vortex growth starts at higher $\lambda\cdot\dot{\gamma}$ values. At the highest regimes examined, the vortex heights of the 2000 and 5000ppm solutions tend to join each other.

The reattachment length of the 100ppm fluid passes from 0.17 (the value for newtonian flow) to 0.29 and it stabilizes at this value. The 500ppm fluid develops larger vortices and X stabilizes at 0.56. For the 5000ppm fluid it covers the whole range from 0.2 to 0.7. The essential difference between flexible and semi-rigid solutions is, thus, the rate of increase of the vortices: With the former ones there is a rapid transition from a newtonian cell size through to larger dimensions and ultimately to unstable rotational and pulsing cell movement. With the latter, vortex growth occurs in a more gradual way.

Respectively, the angle α which is formed by the vortex and the direction of the flow in the entry region shows a monotonic decrease and attains a high regime asymptotic value a_∞.

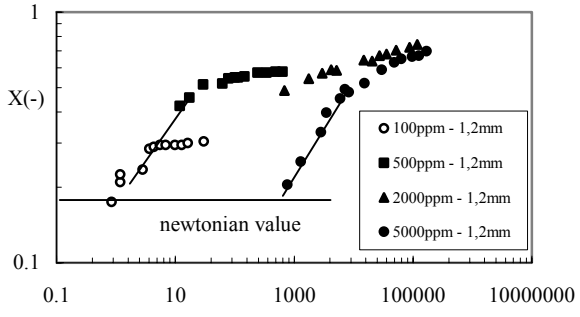

Fig. 5. The reduced reattachment length and entry angle versus deformation rate.

Constant X and α values indicate that the fluid material properties attain constant values in the whole part of the converging zone upstream of the orifice. In a suspension of fibers this should occur when fibers are completely aligned with the flow lines. Our results indicate that, for dilute solutions, complete alignment is achieved for $\lambda\cdot\dot{\gamma}$ from 3 to 50. For semi-dilute solutions, as concentration is increased, neighbouring fibers hinder alignment, so higher $\lambda\cdot\dot{\gamma}$ values are needed.

As previously indicated, inertia crushes the vortices once it becomes important. Boger et al [24] compare experimental observations of the influence of the Reynolds number on X with predictions of Kim et al [25], which match very well: Slightly above *Re*=0.1 vortices start to shrink, and above *Re*=1 this shrinkage becomes considerable. Chiba et al [9] predict a considerable decrease of X for *Re*>1. Our experiments included in general low Reynolds numbers (*Re*<1), with the exception of the 500ppm through the 0.53mm orifice. In this experiment (Fig. 6) vortices start to diminish indeed at *Re*=0.3.

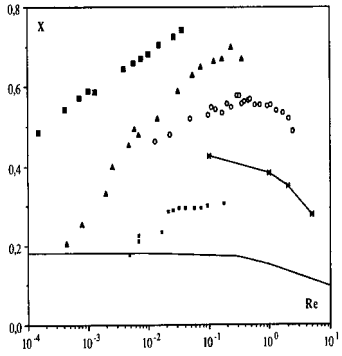

Fig. 6. The effect of inertia on the reduced reattachment length.

5 The extensional viscosity

The orifice flow data were used to calculate the extensional viscosity of the scleroglucan solutions by the method of Binding [23]. According to this analysis, for a constant viscosity fluid and when the pressure drop-flow rate relation is linear, the extensional viscosity is constant. Furthermore, by replacing the shear viscosity η by η_s, following the arguments developed earlier in this paper, it gives:

$$\frac{\eta_E}{3\eta_s}=\frac{9}{32}\left(\frac{P_g}{\eta_s\cdot\dot{\gamma}}\right)^2 \qquad (8)$$

The left member of (8) is the Trouton ratio. On the other hand, the analysis of Batchelor for non-dilute suspensions predicts the extensional viscosity as a function of the shear viscosity of the solvent η_s, the length of the expanded chain L, its equivalent diameter b and the volume concentration $\Phi=n\cdot v$, where v is the volume of a single particle. This analysis ends up with a Trouton ratio:

$$\frac{\eta_E}{3\eta_s}=\frac{\pi L^3\cdot n}{9\log\left(\frac{\pi}{\Phi}\right)}+1 \qquad (9)$$

It is valid if the solutions concentration is such that:

$$b<<\mathrm{H}=(n\cdot L)^{-\frac{1}{2}}<<L \qquad (10)$$

where H is the average distance between the rods in the plane normal to the chain axes.

If the value of L=0.53μm derived under static conditions is used for the estimation of the Trouton

ratio, then the Batchelor analysis gives much lower results for the Trouton ratio than the Binding analysis. Since molecular flexibility is increased by the solvent used, molecular extension should be taken into account. Thus the value of L=1.2μm, (comparable to the values reported in [17] and [19]), corresponding to an extension of about 2.2 was used for this purpose. With this value, the agreement between the Batchelor and the Binding analyses is considerably improved. The values of the Trouton ratio differ by less than 20% for $c \geq 500$ppm (tab. 3).

Table 3. Comparison of the extensional viscosities from the Batchelor and Binding analyses.

c (ppm)	Trouton ratio $Tr=\eta_E/3\eta$ (Binding analysis)	Trouton ratio $Tr=\eta_E/3\eta$ (Batchelor analysis)
100	3.13	1.91
500	7.63	6.86
2000	21.8	26.2
5000	59.8	72.3

Comparable Trouton ratios were found by Khagram et al [26] and Fuller et al [27] for high molecular weight xanthan gum solutions.

A further point in the analysis of Binding can be examined through the values obtained for α.

According to this analysis,

$$tg\alpha = \left(-\frac{dR}{dz}\right) = \left(2\frac{\eta_{E\infty}}{3\eta_s}\right)^{-1/2} \qquad (11)$$

The evolution of tgα with Tr is shown in fig. 7. The scaling law is close to –1/2, the theoretical prediction, which shows coherence of our results with the analysis of Binding.

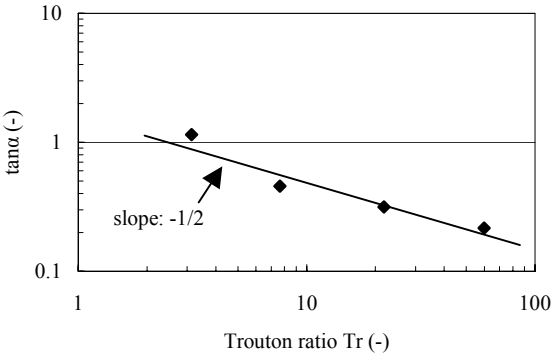

Fig. 7. The entry angle versus Trouton ratio.

6 Conclusions

Experiments on scleroglucan solutions are presented in this paper. In order to avoid inertia during orifice flow, a glucose-syrup was used as a solvent. The shear viscosity of these solutions was first measured. The solutions were found to cover the transition between the dilute and the semi-dilute regimes.

Orifice flow experiments have been performed with these solutions. Scalings of the flow curves and evolution of the flow structure is shown to depend on flow regime and concentration. At low flow regimes where flow strength cannot orient the molecules, solution behaviour is newtonian. Deviation from newtonian behaviour is characterized by a typical Peclet number, the product of the time λ characterising rotational diffusion and the average deformation rate $\dot{\gamma}$. Time scale λ is calculated from the Doi-Edwards theory and is shown to characterise the onset of shear-thinning in shear flow.

For dilute solutions, the onset of viscoelastic effects takes place at $\lambda\dot{\gamma} \cong 3$. For $\lambda\dot{\gamma}$ between 3 to about 10, flow is characterised by a transition regime where the main feature is the evolution of molecular alignment along the streamlines. As a result, the relation between pressure drop and flow rate is linear and the vortex reattachment length as well as the slope of the vortex boundary on the orifice plane become independent of flow rate.

For solutions well into the semi-dilute range, the results indicate that neighbouring molecules hinder alignment, so higher $\lambda\dot{\gamma}$ values are required for molecular orientation. Due to the very high values of λ, only the end of the transition regime and the beginning of the final linear regime were within the range of experimental observations. Results in the literature also cover the final regime, where the vortex length is independent of the flow rate.

Our results for dilute solutions show that, as expected, the vortex re-attachment length varies from the newtonian value at very low flow rates (the higher the length and so the λ value, the lower the $\dot{\gamma}$ where Newtonian behaviour occurs) where molecules are randomly oriented, to a constant value at high flow regimes where molecules are fully aligned. For semi-rigid molecules where molecular orientation is the basic phenomenon, vortex growth is much slower than in solutions of flexible molecules, where in addition important molecular deformation takes place.

The transition regime that separates the newtonian from the asymptotic high flow rate regime, remains to be studied for the semi-dilute solutions. As shown, the basic problem is that, due to important aspect ratios of the semi-rigid macromolecules very high relaxation times characterise the solutions. Observations should be performed at extremely low flow regimes.

The extensional properties were determined by the Binding analysis. This analysis shows that when P_g is linear with q_v for a constant viscosity fluid, the extensional viscosity is constant. Another prediction of the Binding analysis was verified: the variation of the limiting value of the slope of the vortex boundary as the Trouton ratio to the power (-1/2). The analysis of Batchelor predicts also a constant Trouton ratio when molecules are fully aligned with the streamlines. Good agreement is shown to exist between the two theories, provided some molecular

extension - naturally much lower than the one expected for flexible molecules - is considered.

Acknowledgments: The author is grateful to Professors J.-M. Piau of the Laboratoire de Rheologie, Grenoble, France and C. Tzimopoulos of the Polytechnical School of Thessaloniki, Greece, as well as to Dr U. Cartalos for valuable scientific guidance and support.

References:

[1]. R.G. Larson, The rheology of dilute solutions of flexible polymers, *J.Rheol*, 49, 2005, 1-70.

[2]. J.R. Prakash, Rouse chains with excluded volume interactions in steady simple shear flow, *J. Rheol*, 46, 2002, 1353-1380.

[3]. E.J. Hinch and L.G. Leal, The effect of Brownian motion on the rheological properties of a suspension of non-spherical particles, *J of Fluid Mech*., 52, 1972, pp 683.

[4]. E.J. Hinch and L.G. Leal, Time-dependent shear flows of a suspension of particles with weak Brownian rotations, *J. of Fluid Mech*., 57, 1973, pp 753.

[5]. L.G. Leal and E.J. Hinch, Theoretical studies of a suspension of rigid particles affected by Brownian couples, *Rheologica Acta*, 12, 1973, pp 127.

[6]. G.K. Batchelor, The stress generated in a non-dilute suspension of elongated particles by pure straining motion, *J. of Fluid Mech.*, 46, 1971, pp 813-829.

[7]. S.M. Dinh and R.C. Armstrong, A rheological equation of state for semiconcentrated fiber suspensions, *J. of Rheology*, 28, 1984, pp 207.

[8]. G.G. Lipscomb, M.M. Denn, D.U. Hur and D.V. Boger, The flow of fiber suspensions in complex geometries, *J. Non Newt. Fluid Mech.,* 26, 1988, pp 297-325.

[9]. J. Mewis and A.B. Metzner, The rheological properties of suspensions of fibers in Newtonian fluids subjected to extensional deformations, *J Fluid Mech,* 62, 1974, pp 593-600.

[10]. R.J. Binnington and D.V. Boger, Entry flow of semi-rigid rod solutions, *J. Non Newt. Fluid Mech*., 26, 1987, pp 115-123.

[11]. K. Chiba, K. Nakamura and D.V. Boger, A numerical solution for the flow of dilute fiber suspensions through an axisymmetric contraction, *J. Non Newt. Fluid Mech.*, 35, 1990, pp 1-14.

[12]. R.A. Keiller, M. Rallison and J.O. Evans, Sink flows of a suspension of rigid rods: the failure of a similarity solution, *J. Non Newt. Fluid Mech.*, 42, 1992, pp 249-266.

[13]. R.A. Keiller and E.J. Hinch, Corner flow of a suspension of rigid rods, *J. Non Newt. Fluid Mech.*, 40, 1991, pp 323-335.

[14]. A. Mongruel and M. Cloitre, Extensional flow of semi-dilute suspensions of rod-like particles through an orifice, *Phys Fluids*, 7(11), 1995, pp 2546-2552.

[15]. A. Mongruel and M. Cloitre, Axisymmetric orifice flow for measuring the elongational viscosity of semi-rigid polymer solutions, *J. Non Newt. Fluid Mech*., 110, 2003, pp27-43.

[16]. R. Nardin and M. Vincendon, Isotopic exchange study of the scleroglucan chain in solution, *Macromolecules*, 22, 1989, pp 3551-3554.

[17]. T. Yanaki, T. Kojima and T. Norisuye, Triple helix of scleroglucane in dilute aqueous sodium hydroxide, *Polymer J.*, 13, 1981, pp 1135-1143.

[18]. T. Yanaki and T. Norisuye, Triple helix and random coil of scleroglucane in dilute solution, *Polymer J.*, 15, 1983, pp389-396.

[19]. C. Noik and J. Lecourtier, Studies of scleroglucane conformation by rheological measurements versus temperature up to 150°C, *Polymer*, 34, 1993, pp 150-157.

[20]. G. Papaevangelou, Influence de la concentration et de la conformation des chaines sur les ecoulements elongationnelles des solutions de polymers, PhD thesis, *Ins. Nat. Polyt. Grenoble,* France, 1994.

[21]. M. Doi and S.F. Edwards, The theory of polymer dynamics, *Oxford Science publications, Clarendon Press*, Oxford, 1986.

[22]. U. Cartalos and J.M. Piau, Creeping flow regimes of low concentration polymer solutions in thick solvents through an orifice die, *J. Non Newt. Fluid Mech.*, 45, 1992, pp 231-285.

[23]. D.M. Binding, An approximate analysis for contraction and converging flows, *J. Non Newt. Fluid Mech.*, 27, 1988, pp 173-189.

[24]. D.V. Boger, D.U. Hur, R.J. Binnington, Further observations of elastic effects in tubular entry flows*, J. Non Newt. Fluid Mech.*, 20, 1986, pp 31-49.

[25]. M.E. Kim, R.A. Brown and R.C. Armstrong, The roles of inertia and shear-thinning in flow of an inelastic fluid through an axisymmetric sudden contraction, *J. Non Newt. Fluid Mech*., 13, 1983, pp 341-363.

[26]. M. Khagram, R.K. Gupta and T. Sridhar, Extensional flow of xanthan gum solutions, *J. of Rheology*, 29, 1985, pp 191-207.

[27]. G.G. Fuller, C.A. Cathey, B. Hubbard and B. E. Zebrowski, Extensional viscosity measurements of low viscosity fluids, *J. of Rheology*, 31, 1987, pp 235-249.